Sistemas Estelares 2022

Cúmulos de galaxias

Prof. Claudia Scóccola

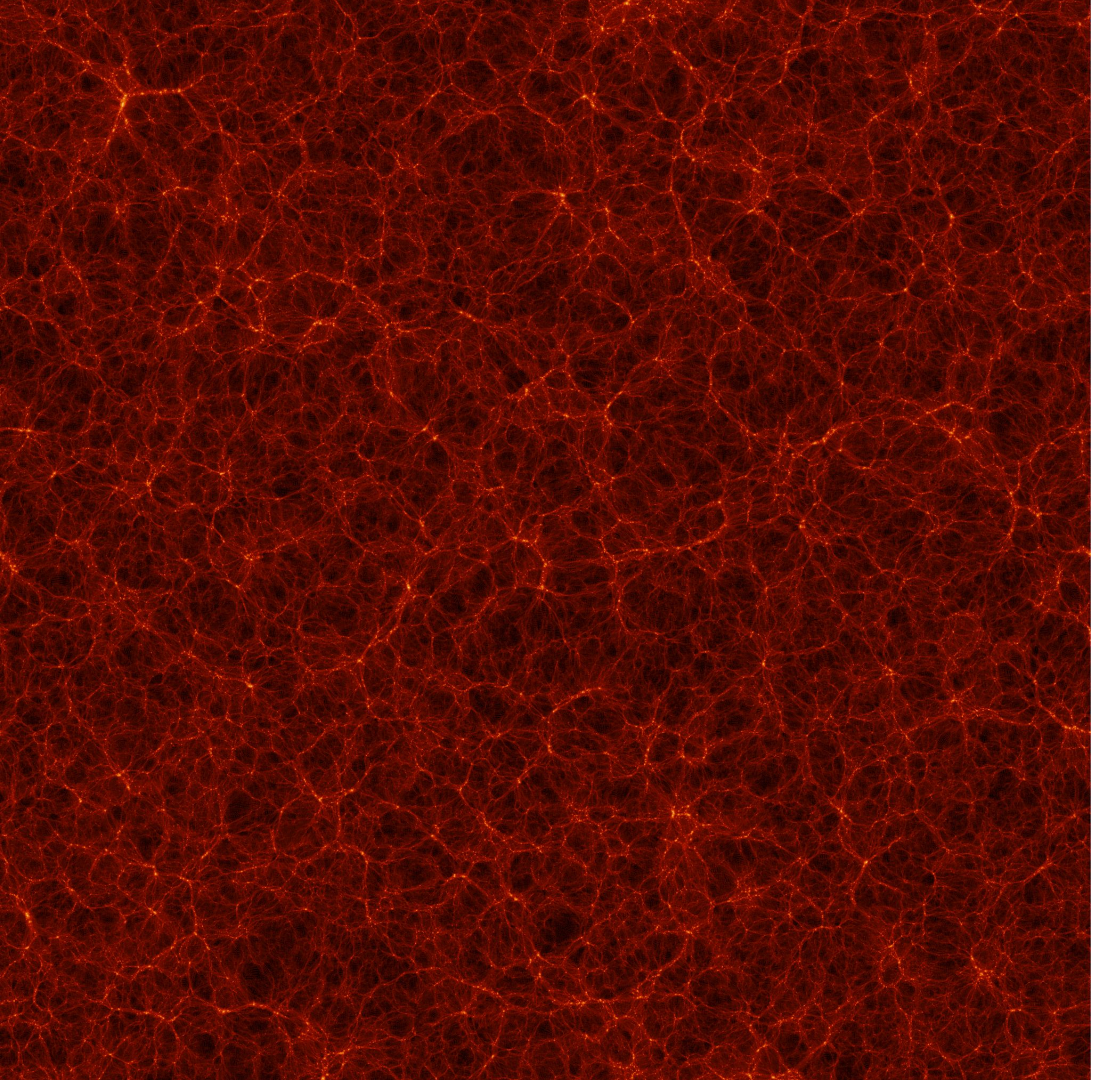

Estructura a gran escala del Universo

Simulación **Big Bolshoi**

Caja de 1 Gpc de lado

http://hipacc.ucsc.edu/Bolshoi/Images.html#bb0

Galaxias en halos (video)

Cúmulos de galaxias

El 50% de las galaxias pertenecen a grupos de galaxias

Los grupos de galaxias y cúmulos son las estructuras más grandes, ligadas gravitatoriamente, que se han formado en el Universo, por el proceso de formación de estructura.

Constituyen las regiones más densas del Universo.

En los modelos de formación de estructura por colapso gravitacional y agregación jerárquica, de materia oscura, las estructuras más pequeñas colapsan primero y luego forman estructuras más grandes, como los cúmulos de galaxias.

Los cúmulos se formaron en los últimos 10 Gyr del Universo.

Los cúmulos a veces se asocian en super-cúmulos.

Formación de un cúmulo de galaxias - IllustrisTNG50

Explicación del video (de la siguiente filmina): Cómo se forman las galaxias? Las simulaciones numéricas nos permiten estudiar la evolución del Universo.
Esta simulación hidrodinámica del conjunto de simlaciones IllustrisTNG se llama TNG50.

La primera parte del video sigue la evolución del gas (mayormente hidrógeno) mientras éste evoluciona para formar galaxias y cúmulos de galaxias desde el Universo temprano hasta hoy. Los colores más brillantes indican el gas moviéndose más rápidamente.
A medida que el Universo evoluciona, el gas cae en los pozos de potencial, las galaxias se forman, giran, chocan y se fusionan galaxies, mientras que los agujeros negros se van formando en los centros de las galaxias y expelen el gas circundante a altas velocidades.
La segunda parte del video, sigue a las estrellas, y muestra como se forma el cúmulo de galaxias, con las galaxias miembros mostrando colas de mareas (tidal tails) y estelas estelares (stellar streams).

https://apod.nasa.gov/apod/ap190226.html


700 kpc
z = 0.13
TNG50

- ❖ Los grupos tienen decenas de miembros, y en promedio tienen unos 0.3 Mpc.
- ❖ Cúmulos ricos: radio promedio ~ 3 Mpc.
- ❖ Super-cúmulos: forman filamentos, contienen algunos cúmulos y muchos grupos. No están en equilibrio hidrostático. El radio promedio es del 30 Mpc.

- ➔ La Vía Láctea pertenece al grupo local.
- ➔ El grupo local tiene al menos 54 miembros.
- ➔ La galaxia más grande del grupo local es Andrómeda.

Grupo local: 1 Mpc de radio.

Super-cúmulo local: VIRGO
Tiene un diámetro de 50 Mpc.

Algunas galaxias satélites de:

← La Vía Láctea

- Sagittarius Dwarf Galaxy
- Large and Small Magellanic Clouds
- Canis Major Dwarf
- Ursa Minor Dwarf
- Draco Dwarf
- Carina Dwarf
- Sextans Dwarf
- Sculptor Dwarf
- Fornax Dwarf
- Leo I
- Leo II
- Ursa Major I Dwarf
- Ursa Major II Dwarf

Andrómeda →

- M32
- M110
- NGC 147
- NGC 185
- Andromeda I
- Andromeda II
- Andromeda III
- Andromeda IV
- Andromeda V
- Andromeda VI
- Andromeda VII
- Andromeda VIII
- Andromeda IX
- Andromeda X
- Andromeda XI
- Andromeda XII
- Andromeda XIII
- Andromeda XIV
- Andromeda XV
- Andromeda XVI
- Andromeda XVII
- Andromeda XVIII
- Andromeda XIX
- Andromeda XX
- Triangulum Galaxy (third-largest galaxy in the local group)
- Pisces Dwarf (unclear if it is a satellite of the Andromeda Galaxy or the Triangulum Galaxy)

LOCAL GROUP

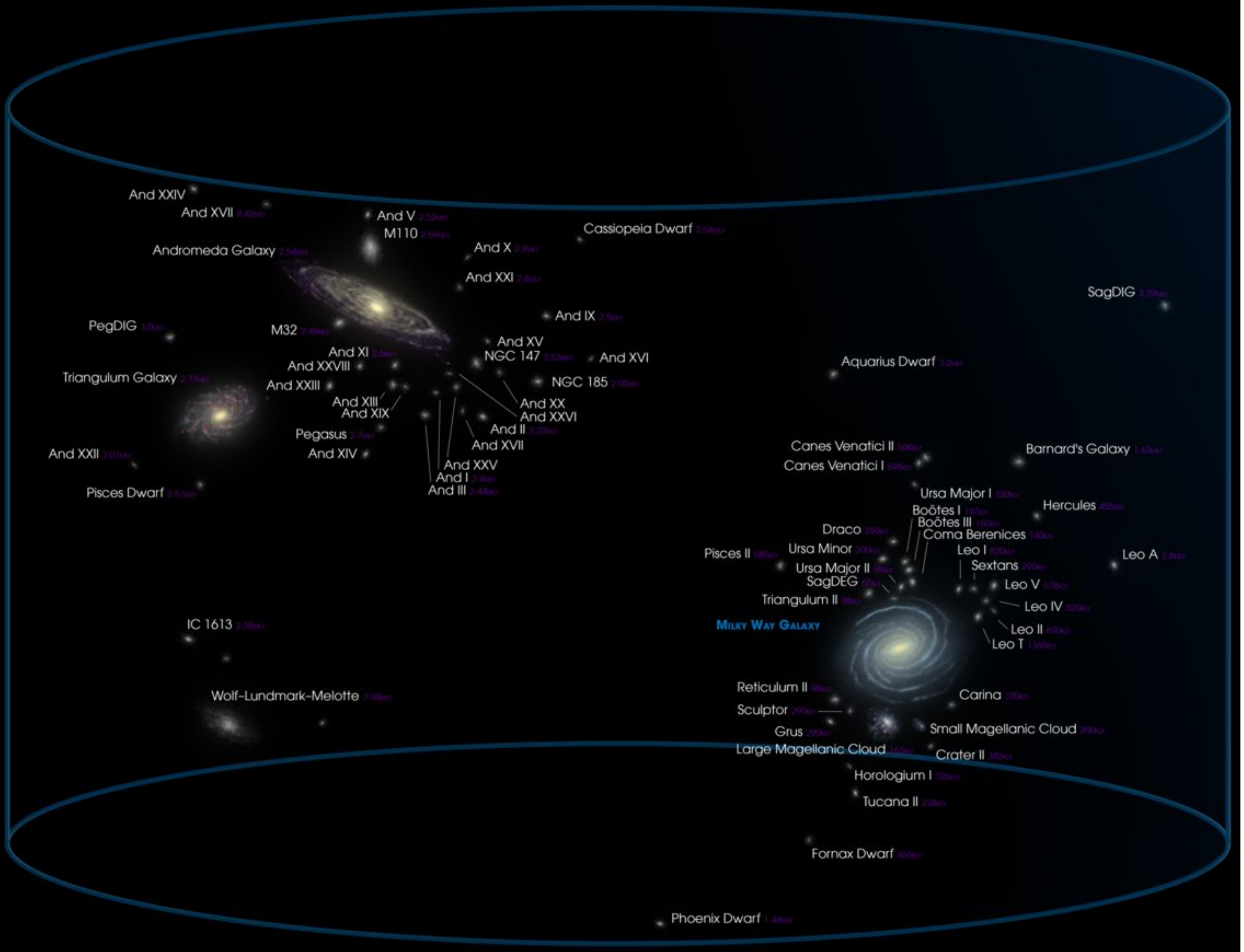

And XXIV
And XVII
And V
M110
Cassiopeia Dwarf
Andromeda Galaxy
And X
And XXI
SagDIG
And IX
PegDIG
M32
And XV
And XI
NGC 147
And XVI
And XXVIII
Triangulum Galaxy
And XXIII
NGC 185
Aquarius Dwarf
And XIII
And XX
And XIX
And XXVI
And II
Pegasus
And XVII
And XIV
And XXII
Canes Venatici II
Barnard's Galaxy
And XXV
Canes Venatici I
And I
And III
Pisces Dwarf
Ursa Major I
Hercules
Boötes I
Boötes III
Draco
Coma Berenices
Ursa Minor
Leo I
Pisces II
Leo A
Sextans
Ursa Major II
SagDEG
Leo V
Triangulum II
Leo IV
IC 1613
Milky Way Galaxy
Leo II
Leo T
Wolf-Lundmark-Melotte
Reticulum II
Carina
Sculptor
Grus
Small Magellanic Cloud
Large Magellanic Cloud
Crater II
Horologium I
Tucana II
Fornax Dwarf
Phoenix Dwarf

Links interesantes:

Estructura a gran escala local:

https://www.universetoday.com/142923/meet-our-neighbour-the-local-void-gaze-into-it-puny-humans/

Golden Webinars – R. Brent Tully - "Galaxy Flows and the Formation of Large Scale Structure"

https://www.youtube.com/watch?v=SR57uHobLpc

Clasificación de cúmulos (clasificación de Bautz–Morgan)

Históricamente, se clasificaban así los cúmulos de galaxias:

● Un **cúmulo tipo I** está dominado por una galaxia brillante, grande y supermasiva (galaxia cD). Por ejemplo, cúmulos Abell 2029 y Abell 2199.

● Un **cúmulo tipo II** contiene galaxias elípticas cuyo brillo relativo al cúmulo es intermedio entre los cúmulos de tipo I y los de tipo III. El Coma Cluster es un ejemplo de tipo II.

● Un **cúmulo tipo III** no tiene miembros sobresalientes, como el cúmulo de Virgo.

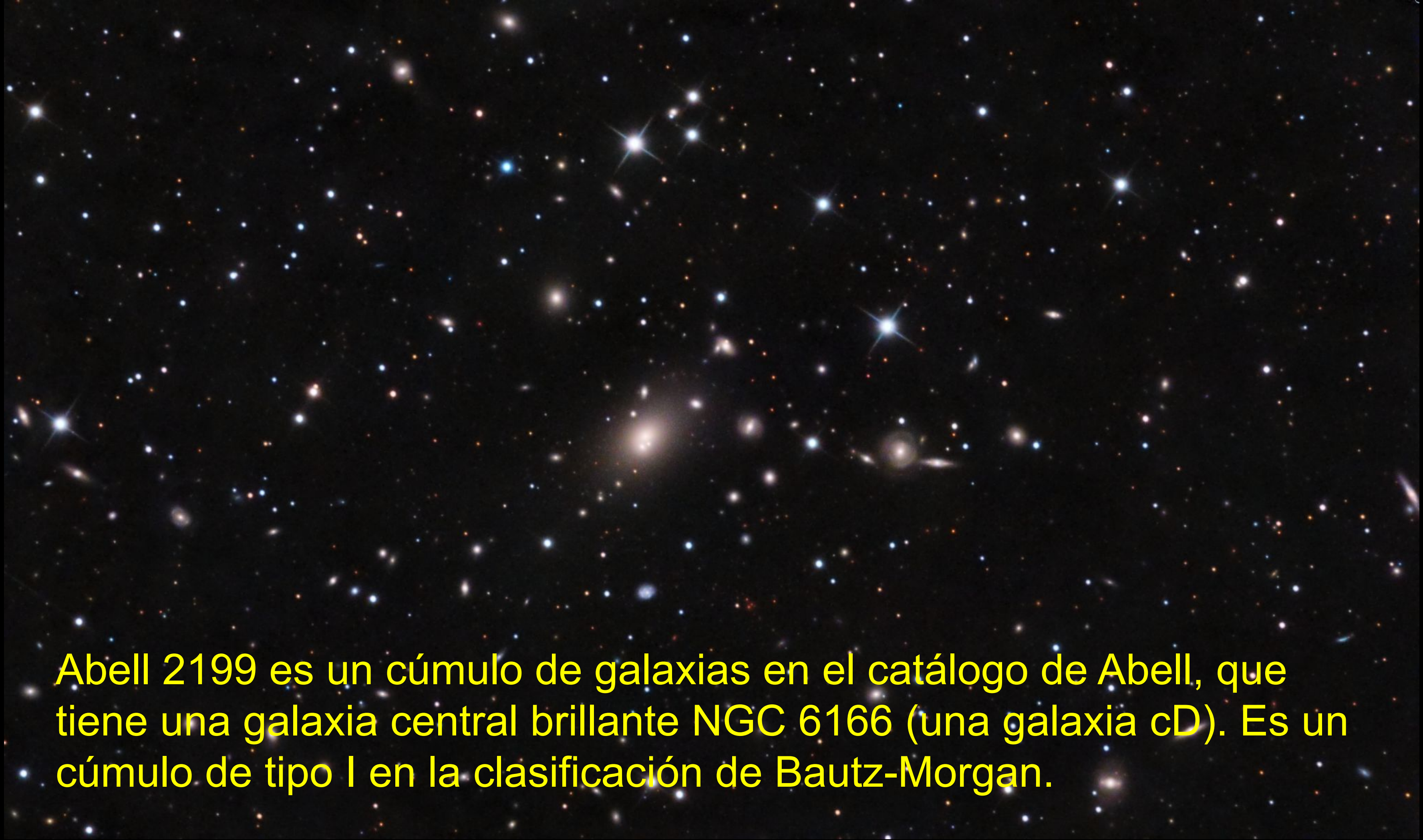
Abell 2199 es un cúmulo de galaxias en el catálogo de Abell, que tiene una galaxia central brillante NGC 6166 (una galaxia cD). Es un cúmulo de tipo I en la clasificación de Bautz-Morgan.

El cúmulo de Coma (Abell 1656) es un cúmulo de galaxias grande que contiene más de mil miembros identificados. Junto con el cúmulo de Leo (Abell 1367), es uno de los mayores cúmulos del supercúmulo de Coma.

Cúmulo de Virgo en la constelación de Virgo. Contiene aprox. 1300 miembros. Está en el centro del supercúmulo de Virgo, del cual el grupo local es un miembro de las afueras del supercúmulo. La masa del cúmulo de Virgo es de $1.2\times10^{15}\ M_\odot$ hasta 8 grados del centro del cúmulo, o hasta un radio de aprox. 2.2 Mpc.

Medio intra-cúmulo:

El gas llena todo el cúmulo, es gas caliente, formado por hidrógeno y helio (gas primordial) y alguna contaminación por parte de las estrellas.

Se estudia en Rayos X.

Catálogos:

- ABELL (1958)
- **"A Catalog of Rich Clusters of Galaxies", Abell, G. O., Corwin, H. G. Jr., and Olowin, R. P. Astrophys. J. Suppl., 1989, vol 70, p1.**
- Catálogo de Zwicky et al (compilado entre los años 1960/1968)
- The Updated Zwicky Catalog (UZC) https://arxiv.org/pdf/astro-ph/9904265.pdf
- http://zmtt.bao.ac.cn/galaxy_clusters/catalogs.html

Diagrama de velocidad radial

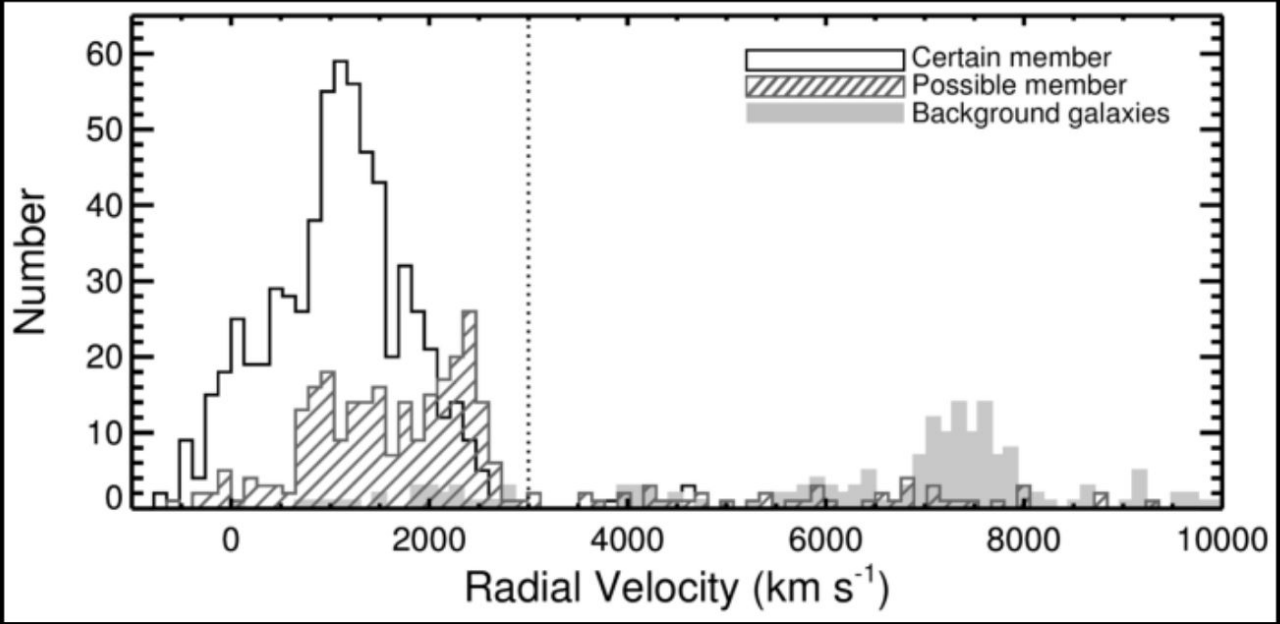

criterio de pertenencia al cúmulo

Determinación de masas: Teorema del Virial

$M = 5 R \sigma^2 / G$

Cúmulo típico:

$R \sim 5$ Mpc

$\sigma \sim 1000$ km/s

$M = 5 \times 10^{15} M_{sun}$

Si calculamos la masa a partir de la luz de las galaxias, obtenemos 5% de la masa del cúmulo.
El gas da cuenta del 20% de la masa del cúmulo

El resto es MATERIA OSCURA.

Las masas de los cúmulos se pueden medir en rayos X y se obtiene el mismo resultado.

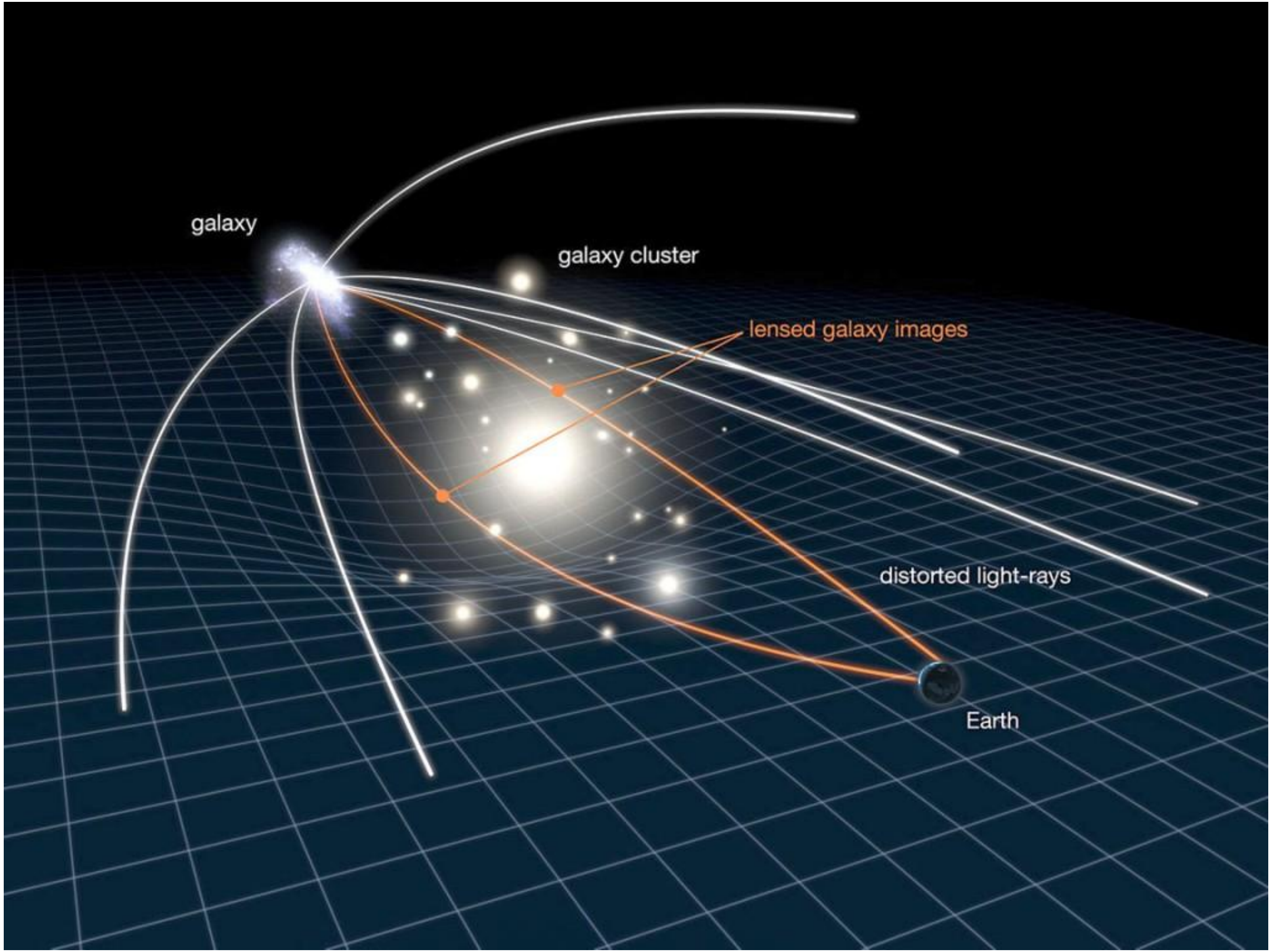

Otro método para estimar la masa de un cúmulo de galaxias es utilizar el efecto de ***lente gravitatoria***.

Efecto Sunyaev-Zeldovich

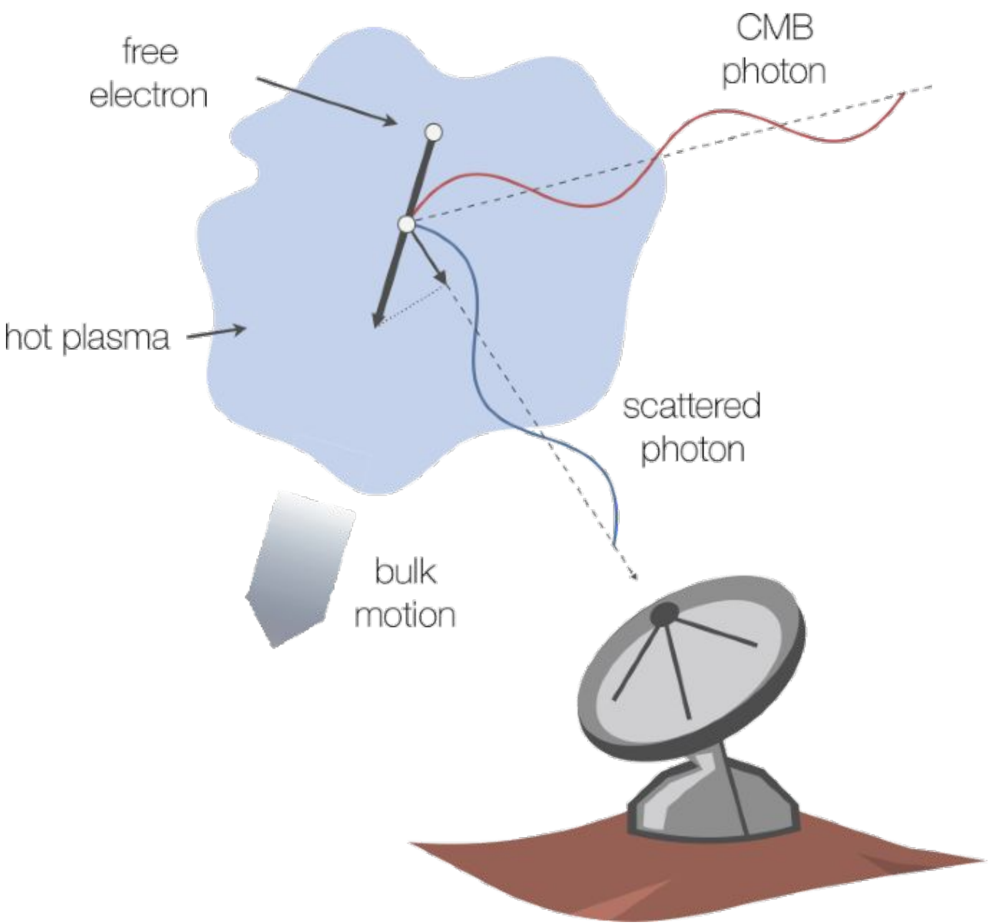

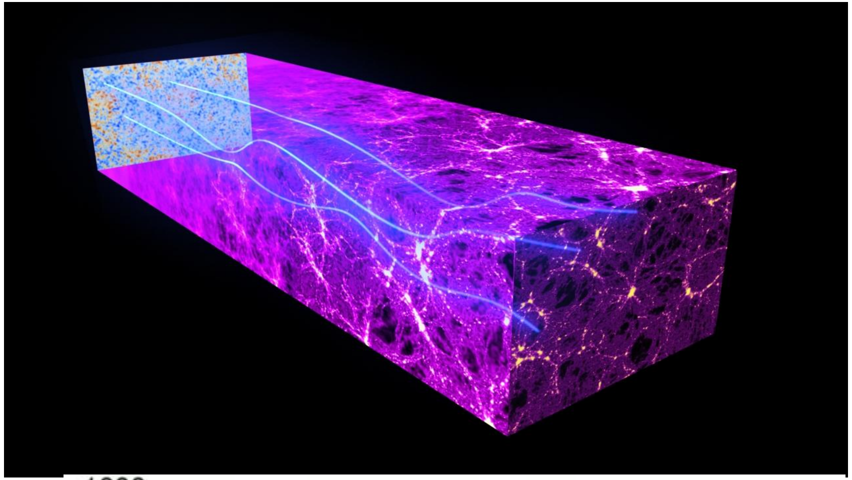

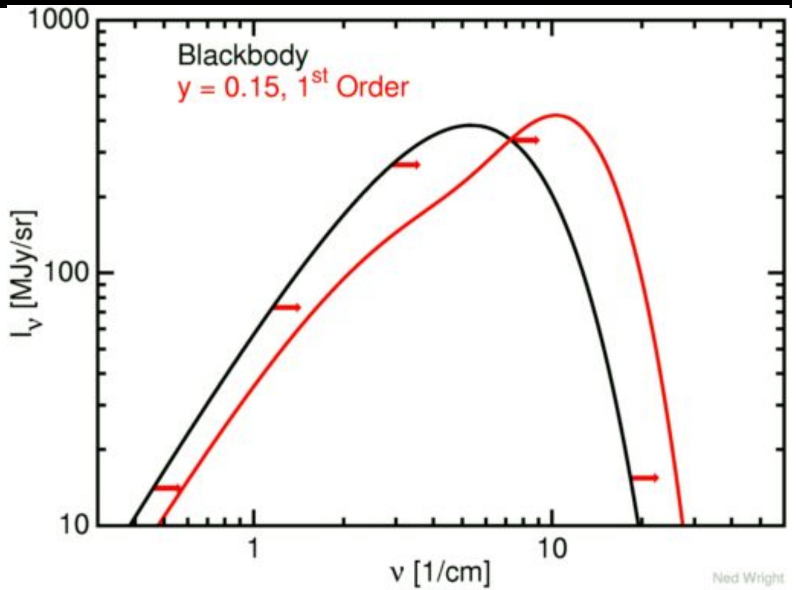

HUNTING GALAXY CLUSTERS WITH PLANCK – THE SUNYAEV-ZEL'DOVICH EFFECT

As the photons of the Cosmic Microwave Background traverse the Universe, they encounter different types of structures which affect their path and energy in various ways, producing a series of observable effects. In the case where the photons pass through a galaxy cluster, a particularly interesting effect ensues: the hot, ionised gas permeating these huge cosmic structures interacts with the photons and modifies their energy distribution in a characteristic way. This phenomenon, known as the Sunyaev-Zel'dovich Effect, represents a powerful tool for detecting galaxy clusters out to high redshift.

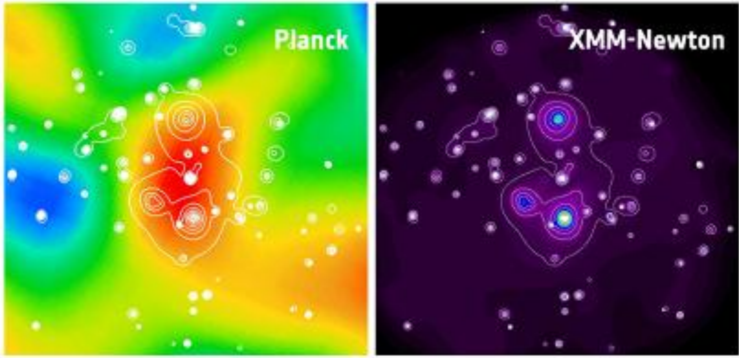

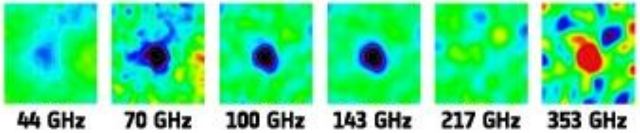

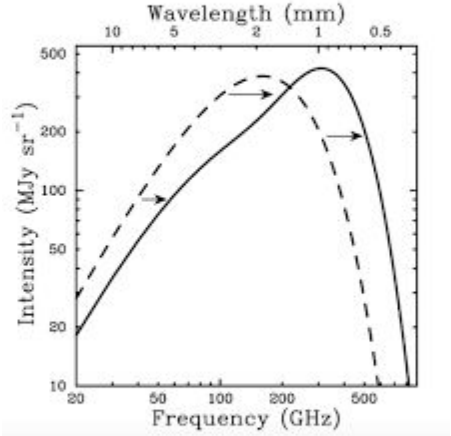

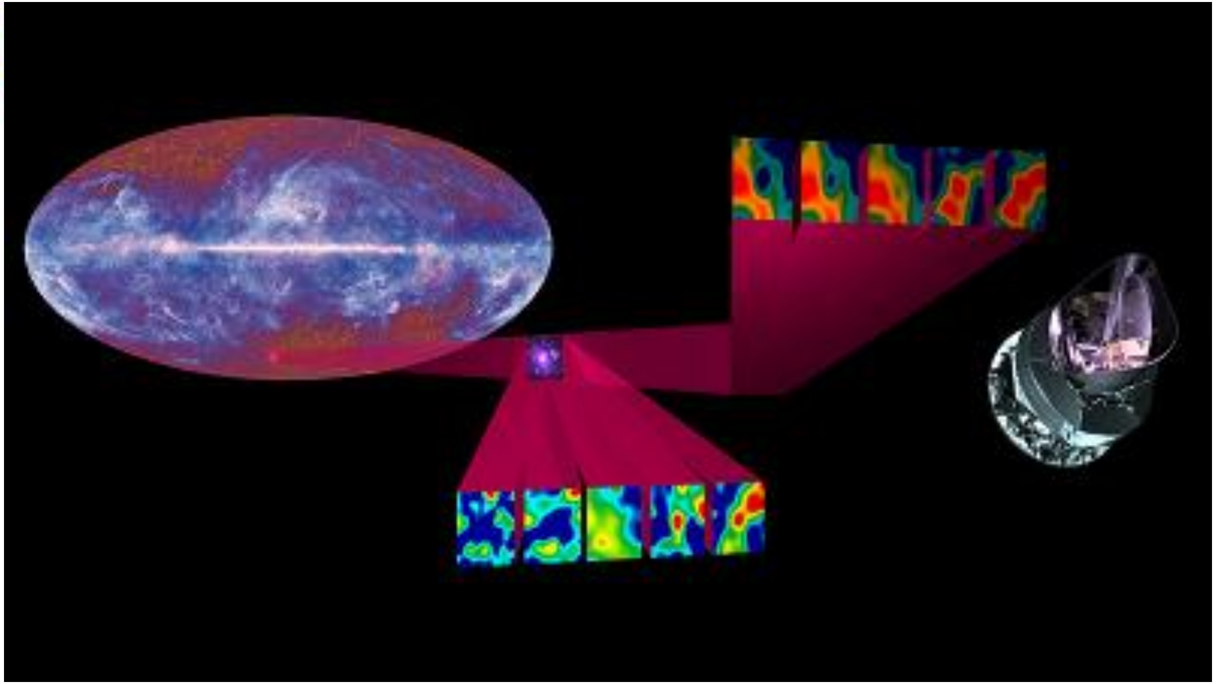

Determinación de distancias

efecto Sunyaev-Zeldovich (SZ)

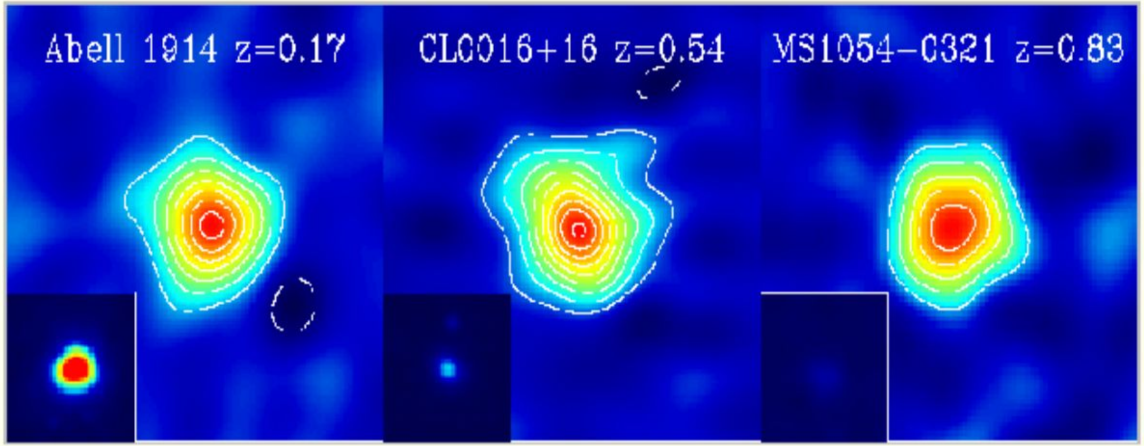

Comparison of the Sunyaev-Zeldovich Effect and X_ray observations of clusters is shown in the image above. Three clusters of differing redshift (z=0.17, 0.54, 0.83) are displayed in the X-ray (in the insets), and in images of the SZ effect. One can note that the X-ray emission falls off with redshift, while the SZ effect hasn't changed much. For this reason, it is essential to use the SZ effect to search for clusters of galaxies.

Mientras que la intensidad del cúmulo de galaxias en rayos X disminuye con la distancia, la intensidad del efecto SZ no depende de la misma.

(b) Thermal Sunyaev-Zeldovich (SZ) Effect

Distortion of the Cosmic Microwave Background (CMB) photon spectrum due to electrons in the CG. (Inverse Compton scattering)

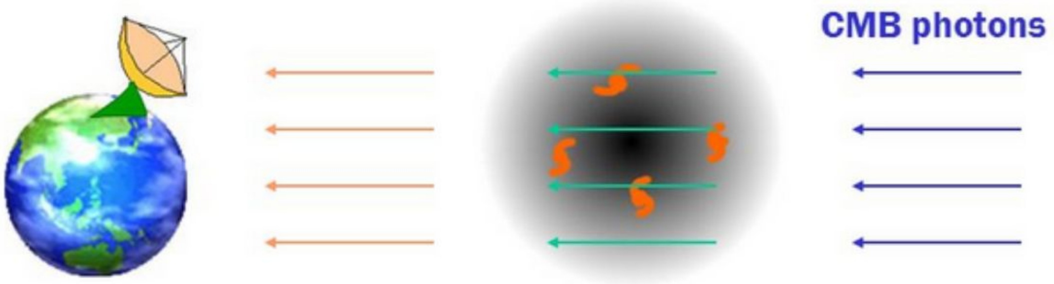

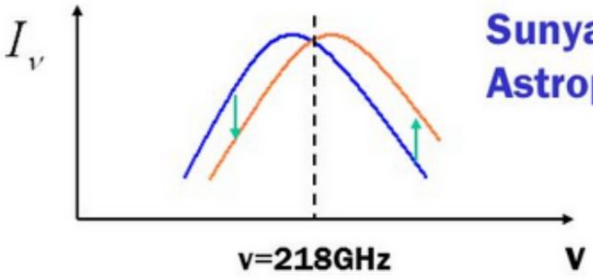

Sunyaev & Zeldovich, Comments Astrophys. Space Phys. 4, 173 (1972) https://iopscience.iop.org/article/10.1086/308662/pdf

THE ASTROPHYSICAL JOURNAL, 533:38–49, 2000 April 10

SUNYAEV-ZELDOVICH EFFECT–DERIVED DISTANCES TO THE HIGH-REDSHIFT CLUSTERS MS 0451.6−0305 AND Cl 0016+16

ERIK D. REESE,[1] JOSEPH J. MOHR,[1,2] JOHN E. CARLSTROM,[1] MARSHALL JOY,[3] LAURA GREGO,[4] GILBERT P. HOLDER,[1] WILLIAM L. HOLZAPFEL,[5] JOHN P. HUGHES,[6,7] SANDEEP K. PATEL,[3,8] AND MEGAN DONAHUE[9]
Received 1999 September 10; accepted 1999 December 2

ABSTRACT

We determine the distances to the $z \simeq 0.55$ galaxy clusters MS 0451.6−0305 and Cl 0016+16 from a maximum-likelihood joint fit to interferometric Sunyaev-Zeldovich effect (SZE) and X-ray observations. We model the intracluster medium (ICM) using a spherical isothermal β model. We quantify the statistical and systematic uncertainties inherent to these direct distance measurements, and we determine constraints on the Hubble parameter for three different cosmologies. For an $\Omega_M = 0.3$, $\Omega_\Lambda = 0.7$ cosmology, these distances imply a Hubble constant of $63^{+12}_{-9}{}^{+21}_{-21}$ km s^{-1} Mpc^{-1}, where the uncertainties correspond to statistical followed by systematic at 68% confidence. The best-fit H_0 is 57 km s^{-1} Mpc^{-1} for an open ($\Omega_M = 0.3$) universe and 52 km s^{-1} Mpc^{-1} for a flat ($\Omega_M = 1$) universe.

Subject headings: cosmic microwave background — cosmology: observations — distance scale — galaxies: clusters: individual (MS 0451.6−0305, Cl 0016+16) — techniques: interferometric

The spherical isothermal β model is given by (Cavaliere & Fusco-Femiano 1976, 1978)

$$n_e(r) = n_{e0}\left(1 + \frac{r^2}{r_c^2}\right)^{-3\beta/2}, \quad (1)$$

where n_e is the electron number density, r is the radius from the center of the cluster, r_c is the core radius of the ICM, and β is the power-law index. With this model, the SZE signal is

$$\begin{aligned} \Delta T &= f_{(x)}\, T_{\rm CMB}\, D_A \int d\zeta\, \sigma_{\rm T}\, n_e\, \frac{k_{\rm B}\, T_e}{m_e\, c^2} \\ &= \Delta T_0\left(1 + \frac{\theta^2}{\theta_c^2}\right)^{(1-3\beta)/2}, \end{aligned} \quad (2)$$

where ΔT is the SZE decrement/increment, $f_{(x)} = [x(e^x + 1)/(e^x - 1) - 4](1 + \delta_{\rm SZE})$ ($f_{(x)} \rightarrow -2$ in the nonrelativistic and Rayleigh-Jeans limits) is the frequency dependence of the SZE with $x = h\nu/kT_{\rm CMB}$, $\delta_{\rm SZE}(x, T_e)$ is the relativistic correction to the frequency dependence, $T_{\rm CMB}$ (=2.728 K;

The X-ray surface brightness is

$$S_{\rm X} = \frac{1}{4\pi(1+z)^4} D_A \int d\zeta \, n_e \, n_{\rm H} \, \Lambda_{e{\rm H}}$$
$$= S_{\rm X0}\left(1 + \frac{\theta^2}{\theta_c^2}\right)^{(1-6\beta)/2}, \qquad (3)$$

where $S_{\rm X}$ is the X-ray surface brightness in cgs units (ergs $\rm s^{-1}\ cm^{-2}\ arcmin^{-2}$), z is the redshift of the cluster, $n_{\rm H}$ is the hydrogen number density of the ICM, $\Lambda_{e{\rm H}} = \Lambda_{e{\rm H}}(T_e, \text{abundance})$ is the X-ray cooling function of the ICM in the cluster rest frame in cgs units (ergs $\rm cm^3\ s^{-1}$) integrated over the redshifted *ROSAT* band, and $S_{\rm X0}$ is the X-ray surface brightness in cgs units at the center of the

One can solve for the angular diameter distance by eliminating n_{e0} (noting that $n_{\rm H} = n_e \mu_e/\mu_{\rm H}$, where $n_j \equiv \rho/\mu_j m_p$ for species j), yielding

$$D_A = \frac{(\Delta T_0)^2}{S_{X0}} \left(\frac{m_e c^2}{k_{\rm B} T_{e0}} \right)^2 \frac{\Lambda_{e{\rm H}0}\, \mu_e/\mu_{\rm H}}{4\pi^{3/2} f_{(x)}^2\, T_{\rm CMB}^2\, \sigma_{\rm T}^2 (1+z)^4} \frac{1}{\theta_c} \times \left[\frac{\Gamma(3\beta/2)}{\Gamma(3\beta/2 - 1/2)} \right]^2 \frac{\Gamma(3\beta - 1/2)}{\Gamma(3\beta)}, \qquad (4)$$

where $\Gamma(x)$ is the Gamma function. Similarly, one can eliminate D_A instead and solve for the central density n_{e0}.

https://arxiv.org/pdf/astro-ph/0512349.pdf

Determination of the Cosmic Distance Scale from Sunyaev-Zel'dovich Effect and *Chandra* X-ray Measurements of High Redshift Galaxy Clusters

Massimiliano Bonamente [1,2], Marshall K. Joy [1], Samuel J. LaRoque [3], John E. Carlstrom [3,4], Erik D. Reese [5] and Kyle S. Dawson [6]

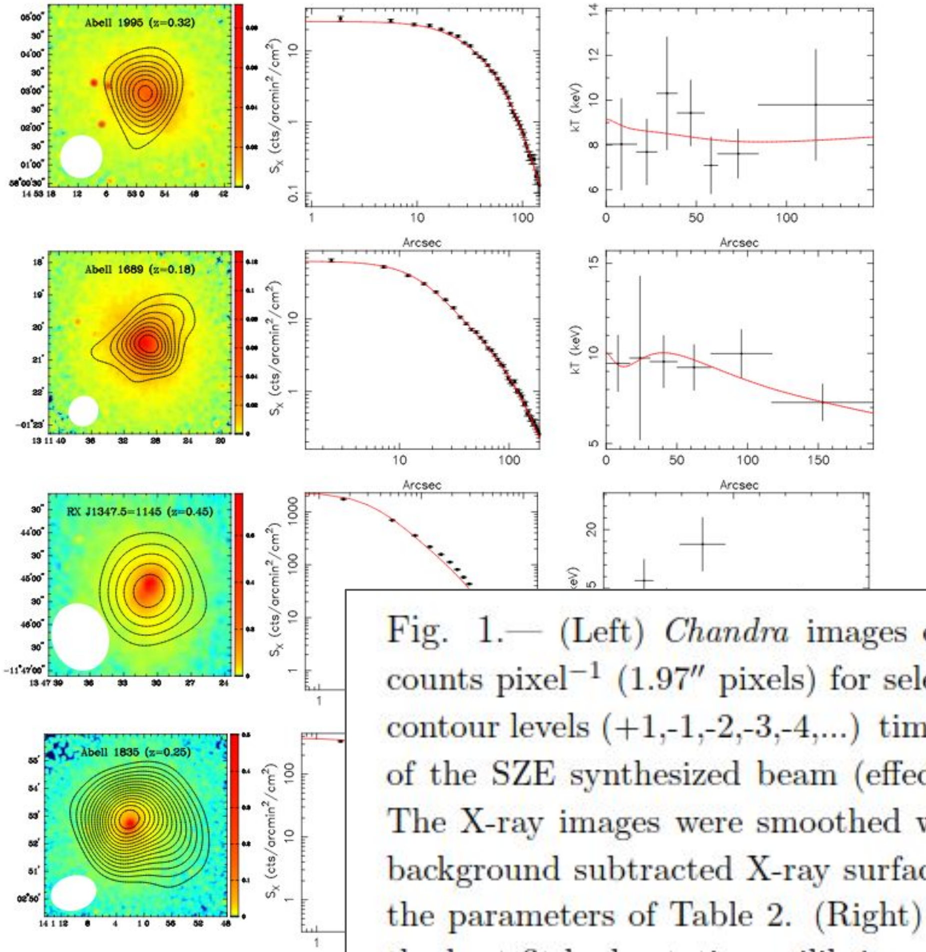

Fig. 1.— (Left) *Chandra* images of the X-ray surface brightness in 0.7-7 keV band in units of counts pixel^{-1} (1.97″ pixels) for selected clusters. Overlaid are the SZE decrement contours, with contour levels (+1,-1,-2,-3,-4,...) times the rms noise in each image; the full-width-at-half-maximum of the SZE synthesized beam (effective point-spread function) is shown in the lower left corner. The X-ray images were smoothed with a $\sigma = 2''$ Gaussian kernel. (Center) Radial profile of the background subtracted X-ray surface brightness; the solid line is the best-fit model obtained with the parameters of Table 2. (Right) Radial profiles of the *Chandra* temperatures, the solid line is the best-fit hydrostatic equilibrium model with the parameters of Table 2.

De la introducción del paper:

Combined analysis of radio and X-ray data provides a method to determine directly the distances to galaxy clusters. Galaxy clusters are the largest gravitationally collapsed structures in the universe, with a hot diffuse plasma ($T_e \sim 10^7 - 10^8$ K) that fills the intergalactic space. Cosmic microwave background (CMB) photons passing through this hot intracluster medium (ICM) have a $\sim 1\%$ chance of inverse Compton scattering off the energetic electrons, causing a small (~ 1 mK) distortion of the CMB spectrum, known as the Sunyaev-Zel'dovich Effect (SZE: Sunyaev & Zel'dovich 1970, 1972; for reviews see Birkinshaw 1999; Carlstrom, Holder, & Reese 2002). The same hot gas emits X-rays primarily through thermal bremsstrahlung. The SZE is a function of the integrated pressure, $\Delta T \propto \int n_e T_e d\ell$, where n_e and T_e are the electron number density and temperature of the hot gas, and the integration is along the line-of-sight. The X-ray emission scales as $S_X \propto \int n_e^2 \Lambda_{ee} d\ell$, where Λ_{ee} is the X-ray cooling function. The different dependences on density, along with a model of the cluster gas, enable a direct distance determination to the galaxy cluster. This method is independent of the extragalactic distance ladder and provides distances to high redshift galaxy clusters.

Historically, the cluster distance has been solved for directly by taking advantage of the different density dependences of the X-ray emission and SZE decrement (e.g., Hughes, Birkinshaw and Arnaud 1991; Reese et al. 2002; Bonamente et al. 2004):

$$S_X \propto \int n_e^2 \Lambda_{ee} dl = \int n_e^2 \Lambda_{ee} D_A d\theta \tag{4}$$
$$\Delta T_{CMB} \propto \int n_e T_e dl = \int n_e T_e D_A d\theta$$

The details of the plasma modelling, such as the numerical integration of the density profile, are included in the proportionality constants of Equations 4. The cluster angular diameter distance $D_A \equiv dl/d\theta$, where θ is the line-of-sight angular size, can be inferred with a joint analysis of SZE and X-ray data by assuming a cluster geometry to relate the measured angular size in the plane of the sky to that along the line of sight. For our adopted spherical geometry, these two sizes are equal.

Our model includes the distribution of dark matter in clusters. The baryonic matter reaches hydrostatic equilibrium in the potential well defined by the baryonic and dark matter components, on a time scale that is shorter than the cluster's age (Sarazin 1988). Under spherical symmetry, this results in the condition

$$\frac{dP}{dr} = -\rho_g \frac{d\phi}{dr} \tag{5}$$

where P is the gas pressure, ρ_g is the gas density and $\phi = -GM(r)/r$ is the gravitational potential due to both dark matter and the plasma. Using the ideal gas equation of state for the diffuse cluster plasma, $P = \rho_g k_B T/\mu m_p$ where μ is the mean molecular weight and m_p is the proton mass, one obtains a relationship between the cluster temperature and the cluster mass distribution:

$$\frac{dT}{dr} = -\left[\frac{\mu m_p}{k_B}\frac{d\phi}{dr} + \frac{T}{\rho_g}\frac{d\rho_g}{dr}\right] = -\left[\frac{\mu m_p}{k_B}\frac{GM}{r^2} + \frac{T}{\rho_g}\frac{d\rho_g}{dr}\right] \tag{6}$$

We combine these hydrostatic equilibrium equations with a dark matter density distribution from Navarro, Frenk and White (1997):

$$\rho_{DM}(r) = \mathcal{N}\left[\frac{1}{(r/r_s)(1+r/r_s)^2}\right] \tag{7}$$

where $\mathcal{N}$ is a density normalization constant and r_s is a scale radius. These model equations are combined with the X-ray and SZE data using a Markov chain Monte Carlo method, described in the following Section.

In Figure 1 the best-fit line (in red) of the X-ray surface brightness is obtained using the density distribution of Equation 1 and the hydrostatic equilibrium model described in this Section. For clusters in which a single β model is an acceptable fit to the X-ray surface brightness (χ^2_r <1.5; see Appendix 2), we simplify the density model of Equation 1 by fixing the parameter $f = 0$. We fit spherically symmetric models to all of the clusters, including those which do not appear circular in X-ray and radio observations, as this approach gives an unbiased estimator of cluster distances when a large sample of clusters is used (Sulkanen 1999).